

***J* and Limit Load Analysis of Semi-elliptical Surface Cracks in Plates under Tension**

Y. Lei & P. J. Budden

British Energy Generation Ltd
Barnett Way, Barnwood
Gloucester GL4 3RS, UK
E-mail: yuebao.lei@british-energy.com

ABSTRACT: *Systematic detailed non-linear finite element (FE) analyses are described for semi-elliptical surface cracks in plates under tension. Limit load solutions are obtained from the FE J results through the reference stress method. The results show that the response of J to load depends on the ratio a/t , where a is the crack depth and t the thickness of the plate. For $a/t \leq 0.5$, J for any position along the crack front can be predicted by the reference stress method using a single limit load value, except for the points very close to the plate surface. For $a/t > 0.5$, J can only be approximately estimated because no single limit load value can be found to satisfy all the FE J solutions along the crack front. The limit load data obtained from this work can be well predicted by a global limit load equation developed by Goodall and Webster.*

INTRODUCTION

In a structural integrity assessment using the R6 procedure [1], the limit load of the defective structure is used to define the L_r parameter. However, because the R6 method is based on the reference stress J -estimation approach, the limit load is not only a parameter for preventing plastic collapse ($L_r < L_r^{max}$) but also a key parameter in assessment against fracture. For a part-through defect, the limit load may be defined according to either the behaviour of the overall plastic deformation of the defective structure (global limit load) or that in the crack ligament (local limit load). The local limit load is always lower than or equal to the global limit load and, therefore, can yield a conservative result in an assessment. However, sometimes it may give an unduly conservative result and lead to unnecessary action.

Previous researchers (e.g. [2-4]) found that the global limit load led to better reference stress estimates of J than did the local limit load. However, the number of cases investigated was limited and the information obtained was not sufficient to give clear guidance for choosing the limit load in

assessments. Moreover, the J solutions could be unreliable because different published results do not agree well and their use can lead to different limit load values for a given geometry.

In the present work, systematic detailed finite element (FE) analyses are performed to generate non-linear J solutions for semi-elliptical surface cracks in plates under tension. To determine the limit load of a cracked plate by the FE method, elastic-perfectly-plastic analysis may be performed and the limit load determined by the load-displacement response of the plate. However, this method is only efficient for determining the global limit load because the local plastic deformation may have little effect on the global displacement. Alternatively, non-linear analysis can be performed to obtain J values and the limit load then determined such that the FE J is well reproduced using the reference stress method [5,1]. The latter approach is used in this work.

METHODOLOGY FOR THE DETERMINATION OF LIMIT LOAD

In the reference stress method, J is related to J_e , the elastic J , and the limit load, P_L , for the defective structure via Eqs. (1) and (2) below [5, 1]:

$$J = J_e \left(\frac{E \mathbf{e}_{ref}}{L_r \mathbf{s}_0} + \frac{L_r^3 \mathbf{s}_0}{2E \mathbf{e}_{ref}} \right), \quad (1)$$

$$L_r = \frac{\mathbf{s}_{ref}}{\mathbf{s}_0} = \frac{P}{P_L(\mathbf{s}_0)}, \quad (2)$$

where \mathbf{e}_{ref} is the reference strain corresponding to a reference stress, \mathbf{s}_{ref} , determined by the stress-strain relationship of the material, \mathbf{s}_0 is the yield or 0.2% proof stress, E is Young's modulus and P is the applied load on the defective structure.

The limit load for a plate with a semi-elliptical surface crack under remote tension may be defined as

$$P_L = 2wt \left(1 - \frac{ac}{wt} \right) \mathbf{s}_0 F(a/c, a/t, c/w), \quad (3)$$

where w and t are the half width and the thickness of the plate, respectively, a is the crack depth and c the half length of the crack (see Fig. 1).

Substituting Eq. (3) into Eq. (2) leads to

$$F(a/c, a/t, c/w) = \frac{\mathbf{s}/\mathbf{s}_0}{L_r \left(1 - \frac{ac}{wt}\right)}, \quad (4)$$

where \mathbf{s} is the remote tensile stress and $P=2wt\mathbf{s}$ has been adopted. Solving for L_r from Eq. (1) with known J and J_e for a loading level \mathbf{s}/\mathbf{s}_0 , the function F can then be obtained from Eq. (4) for a given position on the crack front. J values may be obtained by inelastic FE analysis while J_e may be obtained from elastic stress intensity factor (SIF), K , solutions via

$$J_e = \frac{K^2}{E} (1 - \mathbf{n}^2), \quad (5)$$

where \mathbf{n} is Poisson's ratio. Note that plane strain conditions have been adopted in Eq. (5) because constraint along a surface crack is generally strong. This equation may not apply to the points on the crack front near the plate surface where the constraint could be lower and plane stress conditions may apply.

It should be pointed out that F and hence P_L , obtained from J , may depend on position, \mathbf{j} (Fig. 1), along the crack front, for given a/c , a/t and c/w . The choice of a suitable single value of limit load to represent the whole structure will be discussed later.

FINITE ELEMENT ANALYSIS

3-D FE analysis has been performed using ABAQUS [6]. The dimensions of the plate analysed are shown in Fig. 1 with $w=4c$ and $L=4w$. For all analyses, c was fixed and therefore also w and L . The thickness of the plate, t , was changed according to the ratio a/t for a given a/c . Nine cases ($a/t=0.2, 0.5, 0.8$ and $a/c=0.2, 0.6, 1.0$) have been analysed. The cracked plate was modelled by 8-noded brick elements. Because of symmetry, only a quarter of the plate was modelled. The crack tip was modelled using a focused mesh and J was evaluated at 11 positions along the crack tip in the region $0^\circ \leq \mathbf{j} \leq 90^\circ$, each on 15 contours around the crack tip. J values presented in this paper are the average of all values obtained on the 2nd to 15th contours. The maximum difference between J values obtained on any contour and the

average is less than 5% based on the average value. A Ramberg-Osgood type stress-strain relationship was used in the analyses, that is

$$\mathbf{e}/\mathbf{e}_0 = \mathbf{s}/\mathbf{s}_0 + \mathbf{a}(\mathbf{s}/\mathbf{s}_0)^n \quad (6)$$

where \mathbf{a} and n are a material constant and the strain hardening exponent, respectively, \mathbf{s}_0 is a normalising stress and \mathbf{e}_0 is defined by \mathbf{s}_0/E . In this work, the 0.2% proof stress has been used as \mathbf{s}_0 . For all analyses, $\mathbf{a}=1$, $E/\mathbf{s}_0=500$ and $n=0.3$ were used. Two n values, 5 and 10, were examined. In all the analyses, small strain isotropic hardening was used with the Mises yield criterion.

RESULTS AND DISCUSSION

The method described in Section 2 has been used to evaluate limit loads at 11 positions along the crack front. The normalised limit load, $F(a/c, a/t, c/w)$, obtained from the reference stress method for selected cases, is plotted in Fig. 2 against the normalised load level. Each curve in Fig. 2 represents the limit load values needed to reproduce the FE J at a position on the crack front, \mathbf{j} , under various load levels using the reference stress method. Results for all other cases analysed can be found in [7].

Firstly, cases for $a/t \leq 0.5$ (Figs. 2(a) and (b)) are examined. From Fig. 2(a), in the region $\mathbf{s}/\mathbf{s}_0 > 0.8$, all the curves are horizontal, parallel to each other and almost collapse to one line, except for $\mathbf{j} = 0$. This indicates that a unique limit load value is sufficient to predict J for any point along the crack front except for points very close to the plate surface. In the region $\mathbf{s}/\mathbf{s}_0 < 0.8$, the curves scatter into a band. This means that the response of inelastic J to load varies at different points along the crack front in this region and a limit load value different from that in the region $\mathbf{s}/\mathbf{s}_0 > 0.8$ is required to reproduce the FE J values. However, in the small-scale yielding region, J_e dominates and the total J is not sensitive to the value of the limit load. Therefore, limit load values determined in the region $\mathbf{s}/\mathbf{s}_0 > 0.8$ can also be used to predict J for the lower loading levels without introducing significant error. Similar results can be found from other cases with $a/t \leq 0.5$, e.g. Fig. 2(b) where $a/t = 0.5$ and $a/c = 1.0$.

The cases where $a/t = 0.8$ (see Figs. 2(c)) are next discussed. From Fig. 2(c), it is clear that in the region $\mathbf{s}/\mathbf{s}_0 > 0.8$ all curves are approximately parallel to each other but are scattered into a band. This means that the

response of J to load varies at different points along the crack front. Therefore, a different limit load value is necessary for each position along the crack front to reproduce the FE J values using the reference stress method.

The trends in Fig. 2 may be explained by examining the variation of J/J_e with the crack front position, \mathbf{j} . The FE J results can be expressed as follows via a calibration factor h_1 for a given material and geometry:

$$J(\mathbf{j}) = J_e(\mathbf{j}) + \mathbf{a}e_0\mathbf{s}_0t h_1(\mathbf{j})(\mathbf{s}/\mathbf{s}_0)^{n+1}, \quad (7)$$

where J_e can be obtained from the SIF, K , via Eq. (5). For a given geometry, K for a semi-elliptical surface crack in a plate under tension may be expressed as

$$K(\mathbf{j}) = \mathbf{s} \sqrt{\mathbf{p}a} f(\mathbf{j}), \quad (8)$$

where f is a geometry-dependent factor. Using Eqs. (7), (8) and (5), J/J_e can be expressed as a function of \mathbf{j} :

$$\frac{J(\mathbf{j})}{J_e(\mathbf{j})} = 1 + \frac{\mathbf{a}(\mathbf{s}/\mathbf{s}_0)^{n-1} h_1(\mathbf{j})}{\mathbf{p}(a/t)(1-n^2) f^2(\mathbf{j})}. \quad (9)$$

From Eq. (9), the variation of J/J_e is determined by the ratio $h_1(\mathbf{j})/f^2(\mathbf{j})$ for a given geometry and material. Using factors f and h_1 obtained from FE analyses in [7], the variation of $h_1(\mathbf{j})/f^2(\mathbf{j})$ with normalised \mathbf{j} is shown in Fig. 3 for cases when $n=5$.

For $a/t \leq 0.5$ (see Figs. 3(a) and (b)), the values of $h_1(\mathbf{j})/f^2(\mathbf{j})$ for $\mathbf{j}/(\mathbf{p}/2) < 0.2$ are much lower than those for other positions. For $\mathbf{j}/(\mathbf{p}/2) \geq 0.2$, $h_1(\mathbf{j})/f^2(\mathbf{j}) \approx \text{constant}$ and, by comparing Eqs. (1) and (9), this enables J to be estimated for any position along the crack front in this region by the reference stress method with a single value of limit load. For $a/t = 0.8$ (see Fig. 3(c)), the value of $h_1(\mathbf{j})/f^2(\mathbf{j})$ varies with crack tip position, \mathbf{j} . It is not possible to predict J for all crack front positions with one limit load value in this case. This is why a large scatter is seen in Fig. 2(c).

LIMIT LOAD DETERMINED FROM FE RESULTS

The limit load is a parameter characterising the behaviour of the whole structure. However, for a given crack geometry, the limit load values obtained from the reference stress method for different positions along the crack front are not always consistent with each other (e.g. Fig. 2(c)). A single value of the limit load may nevertheless be determined from the FE results using either of two methods. The first one determines the limit load value by considering the lower bound of the scatter band in Fig. 2. The second method determines the limit load value by considering only the point along the crack front with the maximum J . A limit load may be determined such that the maximum J value along the crack front is well predicted via the reference stress method when this limit load value is used. As discussed above, only the data in the region $\mathbf{s}/\mathbf{s}_0 > 0.8$ are used because the limit load values are more relevant to J in the large-scale yielding and post-yield regions than that in the small-scale yielding region.

The normalised limit load values determined from the lower bound of the scatter band (e.g. Fig. 2) are plotted against a/t in Fig. 4(a) and those from the point with the maximum J value in Fig. 4(b). Comparing Figs. 4(a) and (b), it is found that the determination of limit load by the lower bound or from the maximum J has little effect on the data for $a/t \leq 0.5$. However, for $a/t = 0.8$, the lower bound data lead to the factor F being 15% lower than that obtained from the maximum J values. Two available alternative global limit load solutions are plotted in Fig. 4 for comparison, one due to Goodall & Webster [8] and the other due to Sattari-Far [9]. From Fig. 4, the Goodall & Webster equation can predict the data determined from the maximum J values very well but over-estimates the lower bound data by about 15% for deep cracks. The equation proposed by Sattari-Far gives reasonably good prediction for shallow cracks but, clearly, is very conservative for very deep cracks.

CONCLUSIONS

The relationship between limit load and J has been examined by the 3-D finite element (FE) method and the reference stress J -estimation method for semi-elliptical surface cracks in plates under tension. The conclusions drawn from the results are as follows.

1. The response of J to load depends on the ratio a/t . For $a/t \leq 0.5$, J for any position along a crack front can be predicted by the reference stress

method using a single limit load value, except for the points very close to the plate surface. For $a/t = 0.8$, no single limit load value can be found to satisfy all the FE J solutions along the crack front.

2. For all cases analysed, the maximum J value along the crack front may be predicted by using the reference stress method when the global-based limit load equation due to Goodall & Webster is used.
3. The global limit load equation due to Goodall & Webster can predict the limit load data obtained from this work very well. The equation due to Sattari-Far is less accurate and unduly conservative for deep cracks.

REFERENCES

1. R6 (2001) *Assessment of the Integrity of Structures Containing Defects, Revision 4*, British Energy Generation Ltd..
2. Miller, A. G. (1986) *CEGB Report TPRD/B/0811/R86*, 1986.
3. Chell, G. G.(1989) *CEGB Report RD/L/3415/R88*.
4. Kim, Y. J.(2000) *British Energy Report, E/REP/GEN/0010/00*.
5. Ainsworth, R. A.(1984) *Engineering Fracture Mechanics*, **19**, 633-642.
6. ABAQUS (1998) Hibbitt, Karlsson & Sorensen, Inc., Providence, RI.
7. Lei, Y.(2001) *British Energy Report E/REP/ATEC/0015/GEN/01*.
8. Goodall, I. W. and Webster, G. A. (2001) *Int. J. Pres. Ves. & Piping*, **78**, 687-695.
9. Sattari-Far, I. (1994) *Int. J. Pres. Ves. & Piping*, **57**, 237-243.

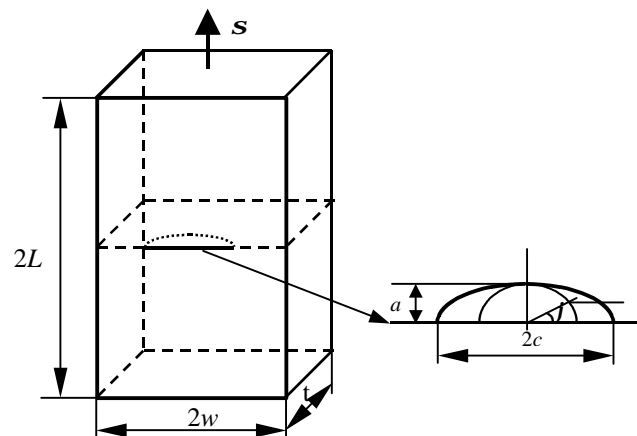
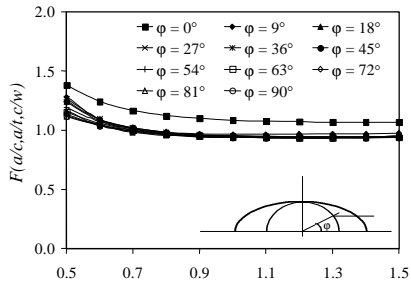
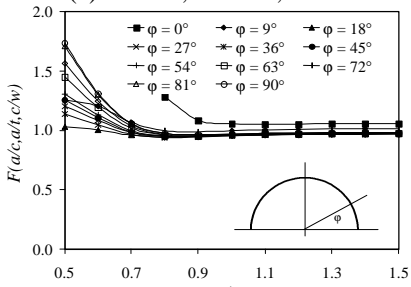


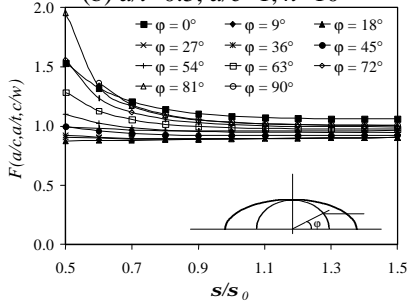
Fig. 1 Geometry of plate with semi-elliptical surface crack under tension



(a) $a/t=0.2, a/c=0.2, n=5$

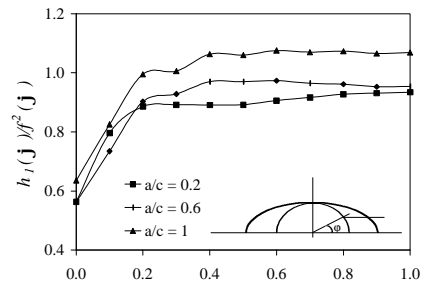


(b) $a/t=0.5, a/c=1, n=10$

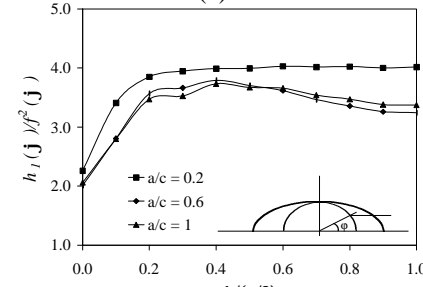


(c) $a/t=0.8, a/c=0.6, n=5$

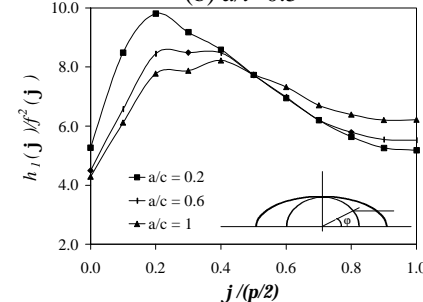
Fig. 2 Normalised limit loads obtained by the reference stress method



(a) $a/t=0.2$

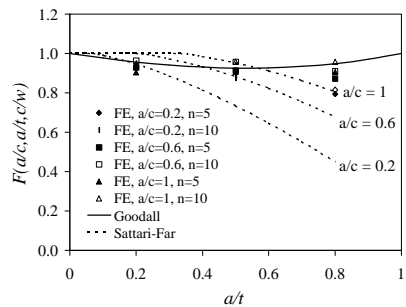


(b) $a/t=0.5$

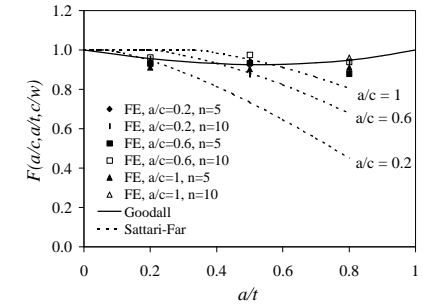


(c) $a/t=0.8$

Fig. 3 Variation of J/J_e along the crack front for $n=5$



(a) From the lower bound of the scatter band



(b) From the maximum J values

Fig. 4 Limit loads obtained from the reference stress method